

Electrical Flow Metering of Blood for Point-of-Care Diagnostics

N. Watkins*, U. Hassan*, W. Rodriguez, and R. Bashir, *IEEE Fellow*

Abstract— We have developed a microfabricated chip that creates a purified white blood cell (WBC) population from whole blood samples and then electrically analyzes the WBCs at the same time as measuring sample volume flow. The flow metering is based on the measurement of the electrical admittance between microelectrodes inside a microfluidic channel. We found that the admittance related to the flow rate linearly. WBC counts which correlated with the flow rate shows how this technique is a viable method in metering and analyzing blood and other biological samples in a point-of-care environment.

I. INTRODUCTION

Accurate, integrated flow metering is essential in point-of-care diagnostics. The introduction of bubbles, variances in microfluidic channel dimensions, fluid dead volume, and errors in infusion methods can contribute to large error between assumed and actual metered sample volumes. These problems are amplified by the fact that extremely small sample volumes are required (~10 μL).

Many have placed their efforts in metering flow rates in the microfluidic regime: integrated optical fiber cantilevers which deflect in proportion to flow speed [1], observing the temperature difference between two points in a channel [2], detecting hydrogen emissions in water with radio frequency plasma-based detectors [3], rapid scanning of fluid movement using laser self-mixing [4], and electrical impedance and admittance-based flow detection in water and ionic solutions [5-7].

We demonstrate a microfluidic chip that processes human whole blood samples to create a purified population of white blood cells (WBCs) in seconds and counts the WBCs at the same time as metering the sample volume flow rate. Cell counting and flow sensing are performed electrically by using the same sensing geometry, resulting in a simple and streamlined design. Our flow rate sensing method is similar to that of Collins and Lee, where there is a positive correlation between flow rate and the electrical admittance found across the microelectrodes [7].

N. Watkins is a postdoctoral research associate at the Micro and Nanotechnology Laboratory (MNTL) at the University of Illinois at Urbana-Champaign, Urbana, IL 61801, USA (phone: 217-333-0751; fax: 217-244-9375; e-mail: watkins7@illinois.edu).

U. Hassan is a Masters student in the Electrical and Computer Engineering Department and MNTL at the University of Illinois at Urbana-Champaign, Urbana, IL 61801, USA (e-mail: uhassan2@illinois.edu).

W. Rodriguez is an Adjunct Professor at Harvard Medical School, and is CEO of Daktari Diagnostics, Cambridge, MA 02140, USA (e-mail: wrodriguez@daktaridx.com).

R. Bashir is a Professor in the Electrical and Computer Engineering Department and is director of MNTL at the University of Illinois at Urbana-Champaign, Urbana, IL 61801, USA (e-mail: rbashir@illinois.edu).

*Equal contribution between N. Watkins and U. Hassan

II. PRINCIPLE AND PROCEDURES

A. Chip Fabrication

Electrodes were patterned on a Pyrex glass substrate by evaporating a 25 nm Ti adhesion layer and 75 nm Pt conduction layer and then lifting off undesired metal using standard photolithographic metal lift-off procedures. Microfluidic channels were created by patterning SU-8 thick negative photoresist (Microchem) as a negative master in which polydimethylsiloxane (PDMS) was poured and cured. Fluidic inlets and outlets were cored into the cured PDMS chips before permanently bonding them to the glass/electrodes layer using oxygen plasma bonding.

B. Microfluidic Sample Preparation

For accurate electrical counting of WBCs, it is necessary to remove all red blood cells (RBCs) from the sample to prevent coincidence events from occurring from the high concentration of red blood cells (~500:1::RBCs:WBCs). Our method uses an on-chip lysing technique, which disrupts the red cell membranes within seconds using a 0.12% (v/v) formic acid and 0.05% (w/v) saponin in DI solution [8]. A quenching solution comprised of concentrated phosphate buffered saline (PBS) and sodium carbonate halts the lysis process to preserve the white blood cells, but allows the saponin detergent to completely disassociate the red blood cell membranes, creating a debris-free white blood cell population. Fig. 1 shows a purified WBC population passing through the counting/flow metering region, described below.

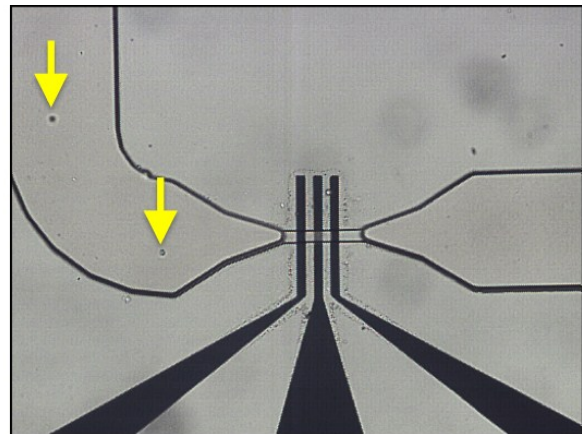


Fig. 1. Counting/flow metering region with three-electrode setup. Transport channels are 200 μm wide and the actual counting/flow metering channel is 15 μm wide. Arrows denote white blood cells have just passed through the counter/metering channel.

C. Electrical Counting of Leukocytes

The purified white blood cell population is then electrically counted using the impedance pulse technique, described in detail elsewhere [9]. Fig. 2 illustrates the electrical setup for enumerating the WBC. A Zurich

Instruments HF2LI lock-in amplifier is used to inject an AC signal into the chip's counter region, which is comprised of two impedance sensing regions, which are balanced by two 10 kΩ resistors in a Wheatstone bridge configuration. The output signals V_1 and V_2 are subtracted to create a flat baseline signal to increase counting accuracy. Cells are funneled into a single-file line by channels with similar dimensions to the cells and pass through and interrupt the ac electric field, creating a distinct pulse above the baseline noise. Each pulse represents a cell passage event.

D. Electrical Flow Sensing

Fig. 2 also illustrates the electrical configuration used to simultaneously count WBCs and measure total flow speed through the counting channel. V_2 , which varies with flow speed of the conductive blood/lysis/quenching solution mixture, is also input into the lock-in amplifier. This electrical measurement of flow rate through admittance monitoring is well established ([5-7]), but has not been shown in point-of-care applications with simultaneous cell counting with the same sensing geometry.

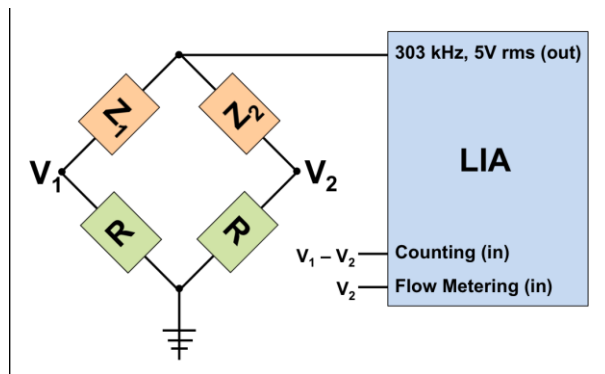


Fig. 2. Circuit diagram of cell counting and flow rate metering system. Z_1 and Z_2 are the impedances found between the first and second electrodes and second and third electrodes, respectively.

III. RESULTS AND DISCUSSION

A. Flow Rate Sensing Calibration

The total flow rate of the on-chip processed blood was varied from 0 $\mu\text{L}/\text{min}$ (static) to 60 $\mu\text{L}/\text{min}$, and the change in V_2 was observed. Fig. 3 shows the relationship between the total flow rate through the counting channel and the signal amplitude of V_2 , which is based on the reference voltage found under static conditions. It is clear that there is a linear relationship between the total flow rate and the amplitude response of V_2 , which agrees with the literature [7].

B. Electrical Counting of Purified WBCs

Purified WBCs were electrically counted at the same time as the flow rate was being measured. Fig. 4 shows the roughly linear relationship between the flow rate and the number of cells that were counted, which came from the same sample. This relationship shows the accuracy of the counter over a range of flow rates. A counting duration of 11 s was used for all flow rates. The discrepancy in cell number for the 40 $\mu\text{L}/\text{min}$ flow rate may have been the result of the blood sample settling in the syringe before injecting it into the chip. Larger counting durations and ensuring no cell

settling beforehand will ensure more accurate cell counts in the future.

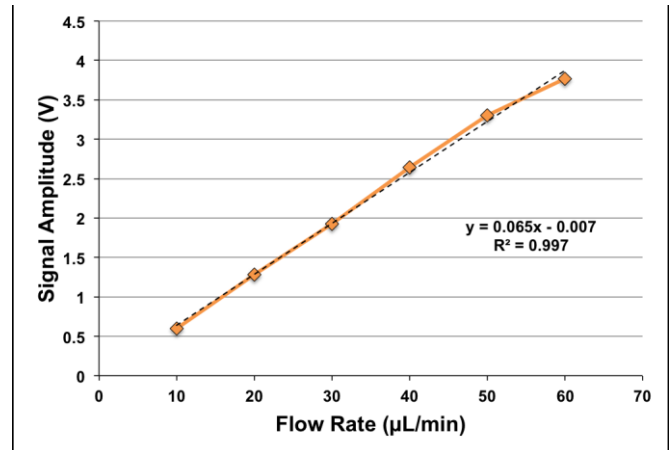


Fig. 3. V_2 signal amplitude comparison with the total flow rate through the counter/metering region.

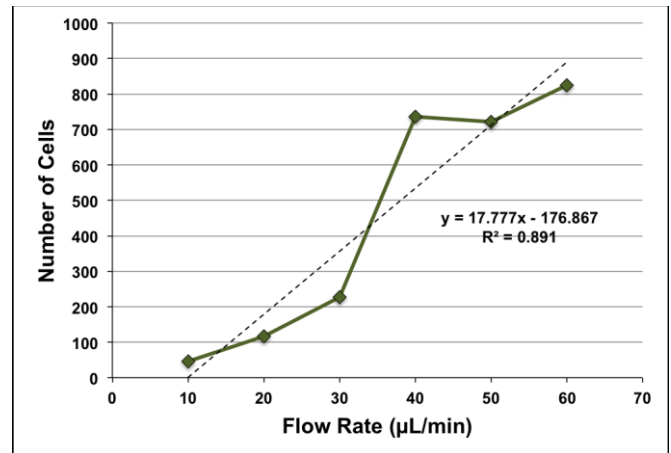


Fig. 4. Cell count vs. total flow rate through the counter/metering region.

Fig. 5 shows the electrical pulse width vs. pulse height distribution found from the same counting/flow sensor experiments—demonstrating how essential cell population data and flow speed data can be obtained simultaneously. Fig. 6 shows how the average pulse width decreases with faster flow rates, which is expected. The standard deviation also decreases, most likely because the pumping system's infusion variance becomes smaller at higher flow rates. Fig. 7 illustrates how the average pulse amplitude decreases as the flow rate increases. The faster flow rates create electrical pulses that have sharper transitions and higher frequency components, which are filtered by the lock-in amplifier's output filter.

IV. CONCLUSION

We have shown the plausibility of simultaneously enumerating on-chip purified WBCs and measuring the sample flow rate with the same electrical sensing geometry. The simplicity of this method will add little additional manufacturing costs and ensure accurate sample metering, both being important for point-of-care devices—especially those targeted for resource-poor regions in the world.

Multiple flow sensors/counters can be designed in parallel on a single chip to increase counting throughput and decrease overall analysis time. The individual flow sensors for each counter would compensate for any sample metering errors seen by the counters. One source of error may be unbalanced fluidic resistances among the different counting branches, which results in differing flow rates in each branch.

Further investigation is needed to ensure the accuracy of this system by comparing the electrically-metered samples to several standards for a range of sample volumes. In addition, chip cell counting accuracy needs to be compared to counts found using industry standard techniques (i.e., flow cytometers or hematology analyzers).

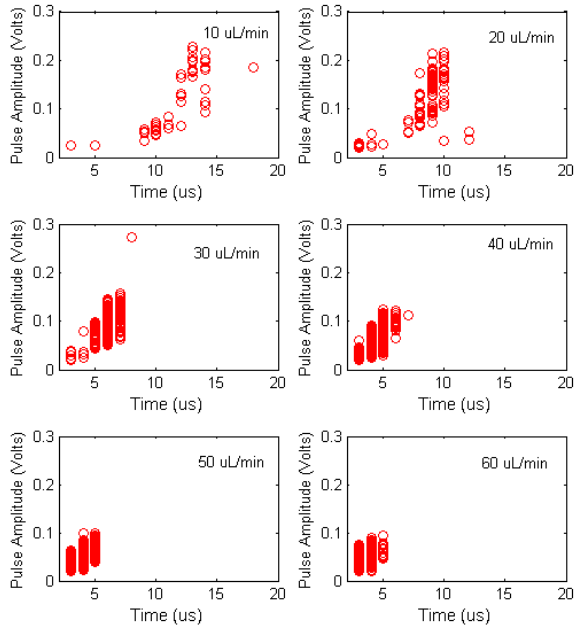


Fig. 5. Scatter plots of pulse amplitude vs. the pulse width for different flow rates.

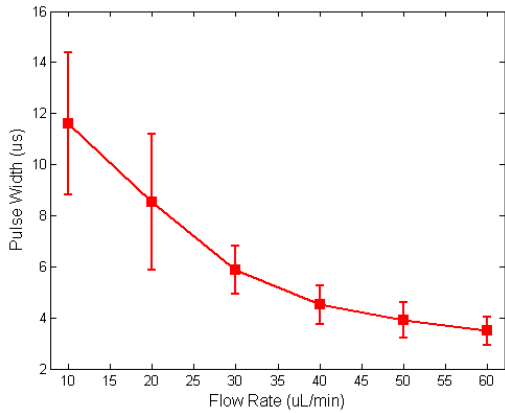


Fig. 6. Pulse width vs. total flow rate for various flow rates.

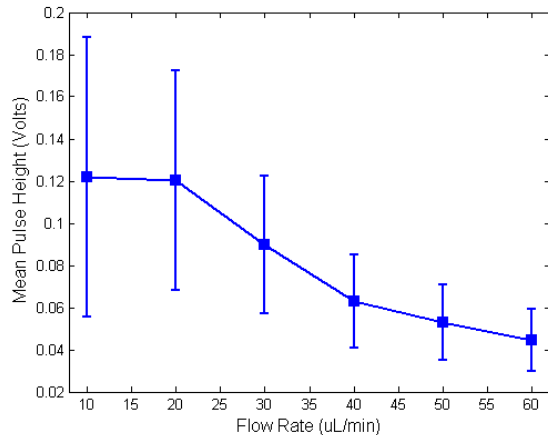


Fig. 7. Pulse height vs. total flow rate for various flow rates.

ACKNOWLEDGMENT

This research was funded by the NSF NSEC at OSU EEC-0914790 and by the University of Illinois at Urbana-Champaign (UIUC).

REFERENCES

- [1] V. Lien and F. Vollmer, "Microfluidic flow rate detection based on integrated optical fiber cantilever," *Lab on a Chip*, 2007, vol. 7, pp. 1352 – 1356.
- [2] H. Ernst, A. Jachimowicz, and G. Urban, "High resolution flow characterization in Bio-MEMS", *Sensors and Actuators A*, 2002, vol. 100, pp. 54 – 62.
- [3] T. Nakagama, T. Maeda, K. Uchiyama, and T. Hobo, "Monitoring nano-flow rate of water by atomic emission detection using helium radio-frequency plasma", *The Analyst*, 2003, vol. 128, pp. 543 – 546.
- [4] R. Kliese, Y. Lim; E. Stefan, J. Perchoux, S. Wilson, and A. Rakić, "Rapid scanning flow sensor based on the self-mixing effect in a VCSEL," 2010 Conference on *Optoelectronic and Microelectronic Materials and Devices (COMMAD)*, pp. 7 – 8, Canberra, Australia, 12 – 15 Dec. 2010.
- [5] H. Yu, D. Li, K. Xu, R. Roberts, N. Tien, "A micro flow sensor for volumetric measurement of conductive fluids," 2010 Conference on the *Advances in Optoelectronics and Micro/Nano-Optics (AOM)*, pp.1 – 5, Guangzhou, China, 3 – 6 Dec. 2010.
- [6] H. Ayliffe and R. Rabbitt, "An electric impedance based microelectromechanical system flow sensor for ionic solutions", *Measurement Science and Technology*, 2003, vol. 14, pp. 1321 – 1327.
- [7] J. Collins and A. Lee, "Microfluidic flow transducer based on the measurement of electrical admittance", *Lab on a Chip*, 2004, vol. 4, pp. 7 – 10.
- [8] C. van Berkel, J. Gwyer, S. Deane, N. Green, J. Holloway, V. Hollis, and H. Morgan, "Integrated systems for rapid point of care (PoC) blood cell analysis", *Lab on a Chip*, 2011, vol. 11, pp. 1249 – 1255.
- [9] N. Watkins, S. Sridhar, X. Cheng, G. Chen, M. Toner, W. Rodriguez, and R. Bashir, "A microfabricated electrical differential counter for the selective enumeration of CD4+ T lymphocytes", *Lab on a Chip*, 2011, vol. 11, pp. 1437 – 1447.